

# Vierendeel mechanism on steel beams with web openings

## Experimental and numerical study

Miguel Romão dos Santos Gomes  
miguel.rgomes22@gmail.com

Civil Engineering Department of Instituto Superior Técnico, October 2017

---

### Abstract

The presented work aims to better understand the behaviour of steel beams with web openings when subject to fracture by the Vierendeel mechanism.

The Vierendeel local bending moment is a consequence of spreading of the shear force through the opening length, causing a high increase of tension and compression at the opening's corners. This effect causes them the corners to plasticize, creating four plastic hinges.

To better understand the behavior of steel beams with web opening, the experimental test of two steel beams was carried out. There were also made numerical models so that the results could be compared.

Lastly two composite beams were design and instrumented to be tested, in order to determine the influence of the concrete slab.

**Keywords** Steel Beams, Web Opening, Vierendeel, Composite Beams.

---

## 1. INTRODUCTION

Civil Engineering is an area fully connected with the search of efficient and economic solutions for structural problems. The problem of allowing service pipes and cables to pass through structural elements without reducing the height of the floor is one of the problems engineers are faced with.

Beams with web openings are a common solution for this type of problem, seeing that cutting an opening through the web is a solution for both mentioned problems. Though it has its advantages, the hole in the web causes a decrease in both shear and bending moment resistance in the cross section in that area.

Besides this decrease in the resistance of the cross section, the area of the beam with the web opening is also subject to local effects, namely the Vierendeel local bending moment.

This local effect is a consequence of the spreading of the shear force at the centre of the opening through its length. This causes a great increase in tension and compression in the sections located at the opening's corner, causing them to plasticize, thus creating a mechanism called Vierendeel mechanism.

## 2. Previous Works

### 2.1 Steel beams with web openings

Throughout the years, many studies, mostly numerical, were made in order to better understand the behaviour of steel beams with a single web opening.

The openings are usually located near the supports, and since most of the beam's shear resistance is supported by the web, the section with the opening is usually the critical section, from which the beam will break.

Besides supporting the bending moment and shear force acting at the centre of the opening, the corner sections are also subjected to a local bending moment, Vierendeel bending moment, represented in figure 1.

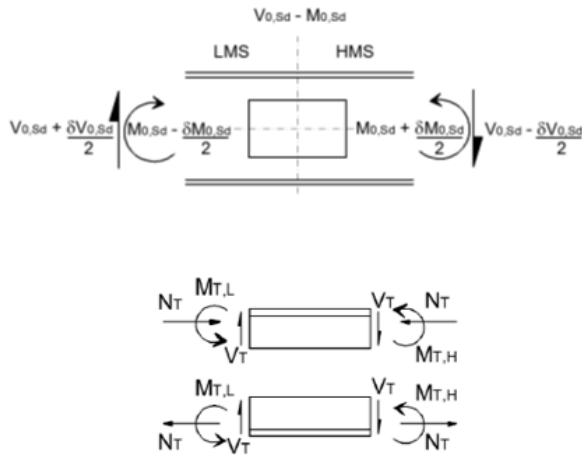


**Figure 1** Vierendeel's local bending moment. Adapted from (Chung & Ko, 2003)

Chung & Ko [1], through an extensive numerical study in 2001, aiming to comprehend the behaviour of steel beams with a single circular opening, concluded that the formation of the first plastic hinge happens on both the upper and lower "T" sections of the low moment side. However, the formation of those hinges happens before the collapse of the beam, making the security approach through that section a conservative one.

The authors also realized that, although the dimensioning the beam through the formation of the plastic hinges in the low moment side leads to conservative results, the high moment side section is not completely plasticized when then beam collapses. Considering this the critical section will lead to non-conservative results.

Chung & Ko [2] made a yet more generalized analysis on steel beams with openings of various shapes and sizes. They verified that the behaviour of the beam with the holed web's behavior is very similar for the different shapes of openings.

It was verified that the lower the bending moment/shear ratio is, the more conditioning the holed section will be. Based on the various numeric models analyzed by the authors, they created simplified generalized interaction curves for the bending moment and shear at the section

with the opening. Here the local actions are accounted as a decrease in the shear resistance of the section.

### 3. Numerical Model

In order to better design the beams that would be tested, numerical models of steel beams and composite beams were made using ABAQUS 6.13 software, since it runs the analysis with non-linearity both geometrical and of the material.

The models were made using 3D elements, with 8 nodes, using full integration (with 4 integration points). The materials were characterized as assigned in the Eurocode, both EN1992-1-1 [3] for the case of the concrete and EN1993-1-5 [4] for the steel.

The steel was modelled using the curve that considers its plastic behaviour, as shown in figure 3.

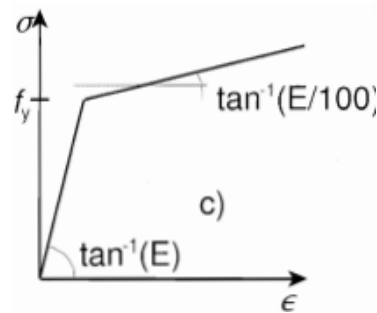


**Figure 2** Steel's stress strain curve used in the modeling of the material. Adapted from EN1993-1-5.

The steel beams were calibrated by comparing them with the beams modelled by Chung & Ko [1], shown in figure 4.

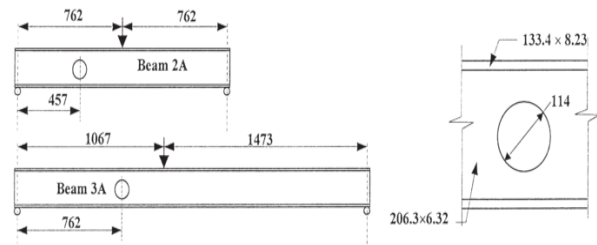


**Figure 3** Beams modelled by Chung & Ko. Adapted from Investigation on Vierendeel's mechanism in steel beams with circular web openings.

As said by the authors, the refining of the mesh didn't need to be too complex. Since the complexity of the mesh is directly connected to

the speed the test runs, only the web opening area needs to be more refined, as shown in figure 5, in beam 2A mesh. The mesh made for beam 3A is very similar to the one shown, only the beam is slightly longer, so it has some more elements.

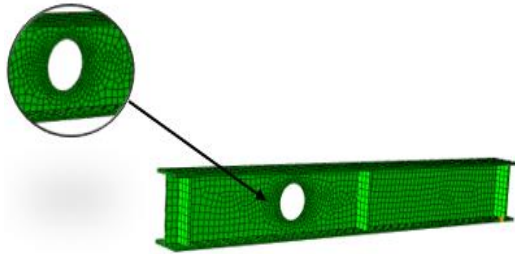


Figure 4 Mesh defined for beam 2A

All that is missing is calibration of the model. This part is made by comparing the results obtained by the model made with results obtained by Chung & Ko [1], as shown in pictures 6 and 7. Since the results for both beams are very similar to the ones modelled by the authors, the calibration of the steel beams is completed.

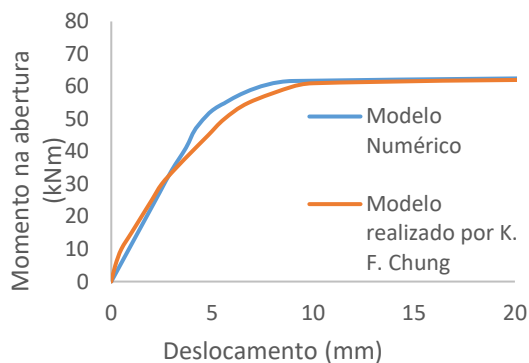


Figure 5 Comparison of the results for beam 2A

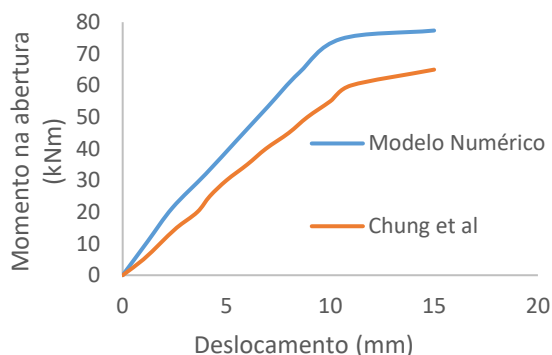


Figure 6 Comparison of the results for beam 3A

The process of calibrating the composite beams was very similar to the calibration of the steel

beams. The material calibrations made for the steel were the same as in that process.

The concrete calibrations were made through a tool facilitated by the program, called Concrete Damaged Plasticity. It simulates both the plastic behavior of concrete when subject to compression, and the loss of strength when subject to tension.

The mesh made was also similar to the ones made for the steel beams, since in this case refining too much wouldn't generate better results. So the option to only refine the mesh in the opening area, as shown in figure 8.



Figure 7 Mesh made for the calibration of the composite beams

The calibration was made by comparing the obtained results with the results of one of Clawson & Darwin [5]'s experimental tests. The comparison of the results is shown in figure 9. Once again, the results obtained were very similar to the ones obtained by the authors, thus completing the model calibration.

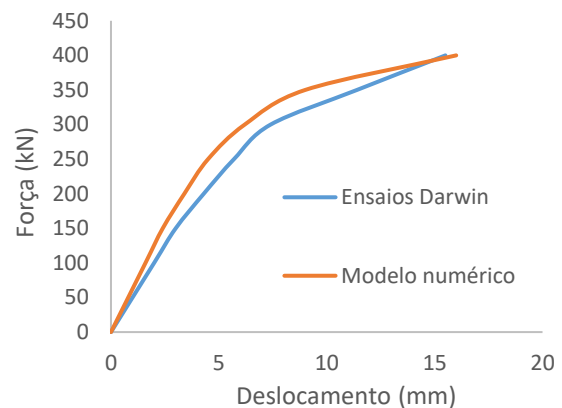


Figure 8 Results for the calibration of the composite beams

#### 4. Design of the steel beams

In this chapter the steel beams that were tested are presented.

Both beams are 4,2m long, with a span of 4m.

Through the numerical analysis carried out by Paulo Bernardino [6], 2013, it was concluded that

the place where the opening has the most influence is at 1/8 of the spam.

The shape of the opening was based on the same study by Paulo Bernardino [9]. It was decided that the opening would be square with a width of 240mm.

#### 4.1 Unreinforced steel beam, V1

Beam V1 was the first to be tested. It was made of a cold rolled steel profile IPE400, detailed in table 1.

**Table 1** IPE400's geometric characteristics

IPE400	
A	8450 mm <sup>2</sup>
A <sub>v</sub>	4269 mm <sup>2</sup>
A <sub>w</sub>	3320 mm <sup>2</sup>
h	400 mm
b	180 mm
t <sub>w</sub>	8,6 mm
t <sub>f</sub>	13,5 mm

The beam is reinforced at both supports and at loads location. The details of the web opening are shown in figure 10.

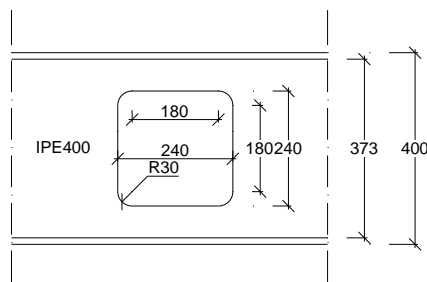


**Figura 9** Web opening's detailing

A numerical study was made, in order to determine if the failure would happen by the desired method.

The results obtain were satisfactory. Figure 11 illustrates the Von Mises stresses obtained through the numeric model.

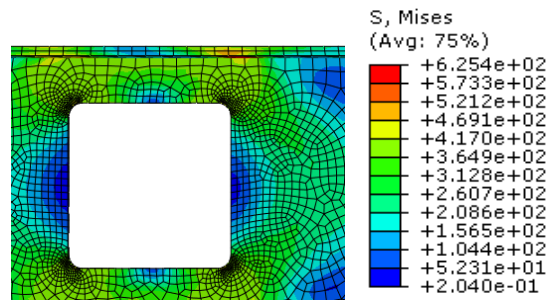


**Figure 10** Von Mises stresses at the opening's corners obtained through the numerical model

It is clear the formation of the four plastic hinges at the corners of the web hole. This confirms failure happens through Vierendeel's mechanism.

#### 4.1 Reinforced steel beam, V2

The second beam to be tested was beam V2. It was also made of a cold rolled steel profile IPE400.

The difference of this beam to beam V1 consisted on the web reinforcement at the perforated section. The detailing of the opening is shown in figure 11

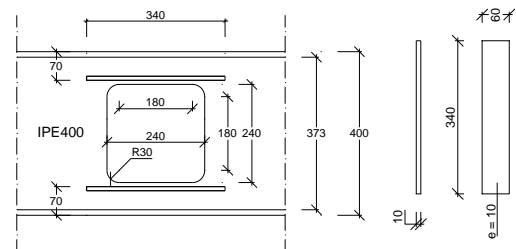


**Figura 11** Detailing of the reinforced opening and the reinforcement

A numerical study was made, in order to determine if the failure would happen by the desired method.

The results obtain were satisfactory. Figure 11 illustrates the Von Mises stresses obtained through the numeric model.

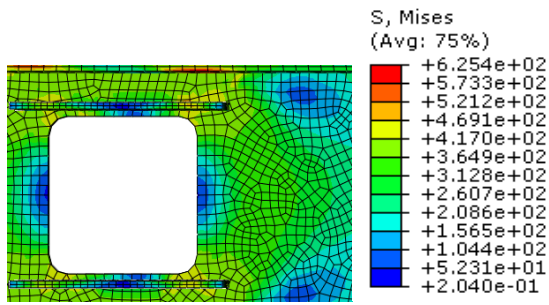


**Figure 12** Von Mises stresses at the opening's corner obtained through the numerical model

It is clear the formation of the four plastic hinges at the corners of the web hole. This confirms failure happens through Vierendeel mechanism.

## 5. Experimental Campaign

In this chapter the experimental tests of two steel beams will be described. The tensile tests made to characterize the materials are also described

The results obtained for each beam are detailed and analysed. The results for both tests are also compared.

### 5.1 Material Characterization

The first step of this campaign is the characterization of the materials. This characterization was made through tensile testing of two probes of steel from the web and two probes of steel from the flanges and one probe of longitudinal reinforcement steel.

The tests were made on LERM at Instituto Superior técnico, according to EN ISO 6892-1 [6] standards.

The results obtained are shown in table 2. The reinforcement probe was removed from the beam after it was tested. The results obtained for this probe were not acceptable, and so they were not considered

**Table 2** Results obtained for materials tested

	$\sigma_{ced}$ (Mpa)	$\sigma_u$ (Mpa)	$\epsilon_u$ (%)
Web	371	483	23
Flanges	346	465	20

## 5.2 Steel Beam without reinforcement, V1

### 5.2.1 Instrumentation of the test

After the beam is conceived, the next step is to instrument the test.

The test was realized on Laboratório de Estruturas e Resistência dos Materiais (LERM) on Instituto Superior Técnico.

The test was made under the closed portico shown in figure 17. The instrumentation of the test is also shown on the same figure, and the details of the instruments are shown in table 2.

There were put transducers in the places with the biggest deflection, in order to control it.

The control of lateral displacement was made through the transducer d7, placed at half span. In the support near the opening the control of horizontal displacement in the direction of the beam was made through the transducer d8.

F1 and F2 refer to the load cells placed between the hydraulic jack. The characteristics of both the jacks and the loads cells are shown in table 2.

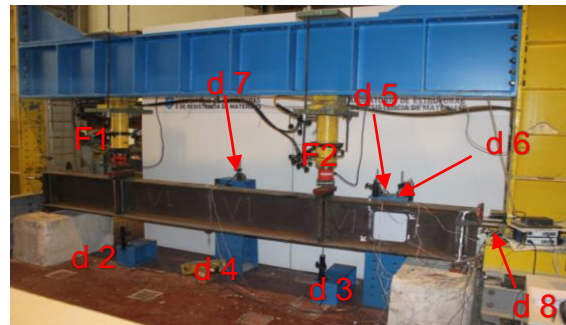


**Figure 13** Portico instrumented for beam V1 test

**Table 3** Characteristics of the instruments for the test of V1

	Length (mm)	Capacity (kN)
Jack 1	-	600
Jack 2	-	600
F1	-	400
F2	-	400
d2	100	-
d3	100	-
d4	500	-
d5	50	-
d6	50	-
d7	50	-
d8	50	-

There were also put strain gauges on the beam. They were put on the maximum stress locations, which are near the opening's corners and on the flanges above and below them. There were also place strain gauges in the flanges at the



middle span, in order to control the stresses on that area. The location of all the strain gauges is shown in figure 14.

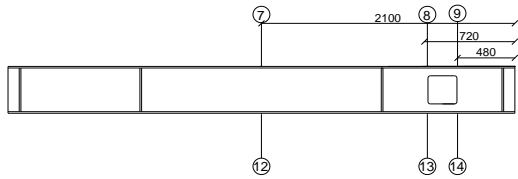


Figura 14 Strain gauges placed on beam V1

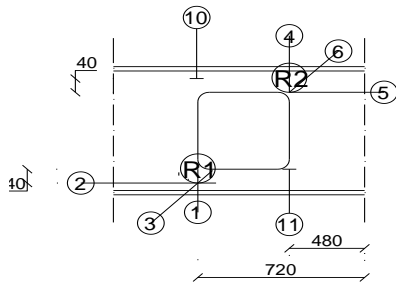


Figure 15 Position of the strain gauges at beam's V1 opening

It's important to refer that strain gauges e1 to e3 and e4 to e6 correspond to rosette strain gauges R1 e R2 respectively. These rosettes were placed at the corners of the opening in order to determine the principal directions of stress, as well as their maximum and minimum value.

### 5.2.1 Experimental test

Beam V1 was tested to failure, which happened by the Vierendeel's mechanism.

The test was run in a load-unload model, with a load increase at each loading cycle. The loading history is illustrated in figure 17.

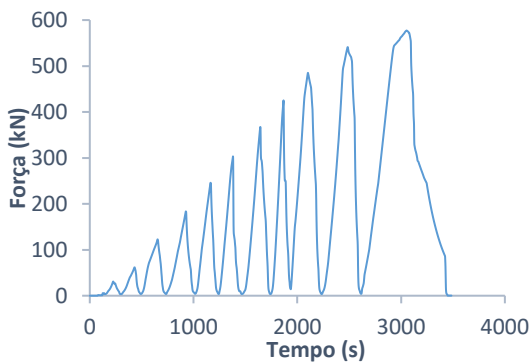


Figure 16 Loading history used for the test of beam V1

At failure, the deformations at the opening were clear. It is perceptible that the corners in which

the local bending moment induces tension, it created wide fractures.

On the other hand, the corners where the local bending moment induces compression, the web buckles outside of its plane. The deformations on the opening are shown in figure 18.

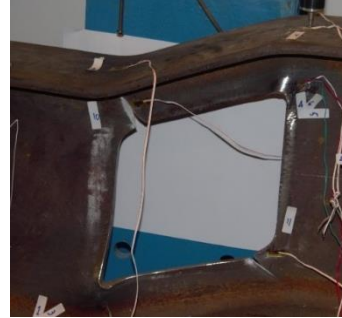


Figure 17 Deformation at the web opening

It is also clear that the rest of the beam is completely linear when it collapses.

Figure 19 illustrates the deformed shape, where it is observable besides the opening, the beam's shape is completely linear.



Figura 18 Beam's final deformed shape

The results registered by the gauges also show that the stress level reaches its peak at the web opening.

The results obtained at the rosettes are shown in figure 19. Rosette R1, placed further from the corner, has a slower growing rate than R2

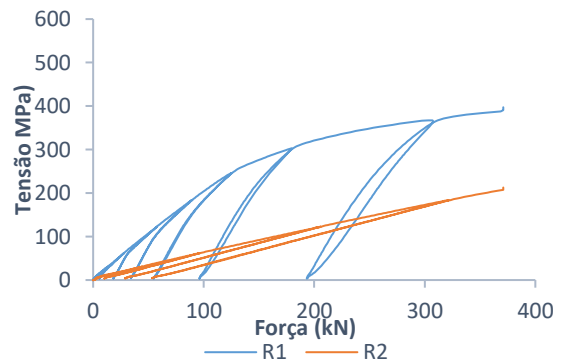


Figure 19 Maximum Compression tensions at both rosettes

### 5.3 Reinforced steel beam, V2

#### 5.3.1 Instrumentation of the test

After the beam is conceived, the next step is to instrument the test.

The test was realized on Laboratório de Estruturas e Resistência dos Materiais (LERM) on Instituto Superior Técnico.

The test was made under a closed portico, similar to the one where beam V1 was tested.

There were put transducers in the places with the biggest deflection, in order to control it.

The control of lateral displacement was made through the transducer d7, placed at half span. In the support near the opening the control of horizontal displacement in the direction of the beam was made through the transducer d8.

F1 and F2 refer to the load cells placed between the hydraulic jack. The characteristics of both the jacks and the loads cells are shown in table 3.

**Table 4** Characteristics of the instruments for the test of V1

	Length (mm)	Capacity (kN)
Jack 1	-	600
Jack 2	-	600
F1	-	400
F2	-	400
d2	50	-
d3	100	-
d4	500	-
d5	100	-
d6	50	-
d7	50	-
d8	50	-

There were also put strain gauges on the beam. They were put on the maximum stress locations, which are near the opening's corners and on the flanges above and below them. There were also place strain gauges in the flanges at the middle span, in order to control the stresses on that area. The location of all the strain gauges is shown in figure 14.

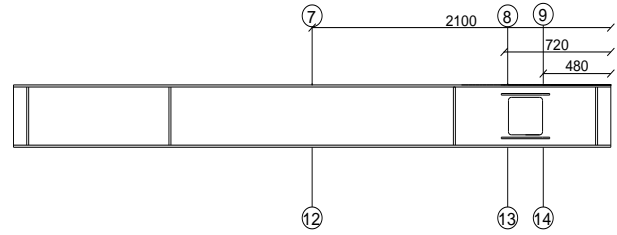


**Figure 20** Strain gauges placed on beam V1

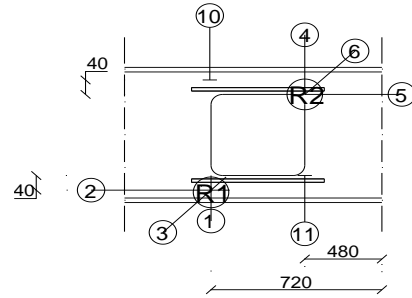


**Figure 21** Position of the strain gauges at beam's V1 opening

It's important to refer that strain gauges e1 to e3 and e4 to e6 correspond to rosette strain gauges R1 e R2 respectively. These rosettes were placed at the corners of the opening in order to determine the principal directions of stress, as well as their maximum and minimum value.

#### 5.3.2 Experimental test

Beam V2 was tested to failure, which happened by the Vierendeel's mechanism.

The test was run in a load-unload model, with a load increase at each loading cycle. The loading history is illustrated in figure 17.

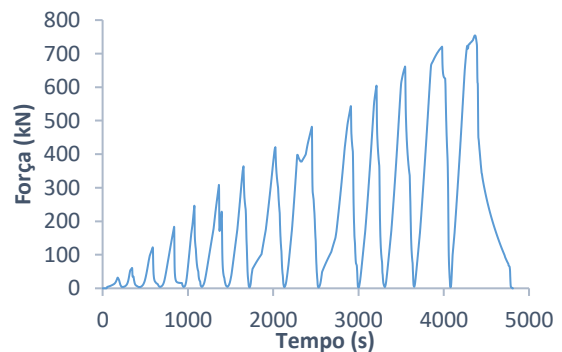


**Figure 22** Loading history used for the test of beam V1

At failure, the deformations at the opening were clear. It is perceptible that the corners in which

the local bending moment induces tension, it created wide fractures.

On the other hand, the corners where the local bending moment induces compression, the web buckles outside of its plane. The deformations on the opening are shown in figure 18.



**Figure 23** Deformation at the web opening

It is also clear that the rest of the beam is completely linear when it collapses.

Figure 19 illustrates the deformed shape, where it is observable that besides the opening, the beam's shape is completely linear.



**Figure 24** Beam's final deformed shape

The results registered by the gauges also show that the stress level reaches its peak at the web opening.

The results obtained at the rosettes are shown in figure 19. Stresses at rosette R1, placed further from the corner, have a slower growing rate than R2.

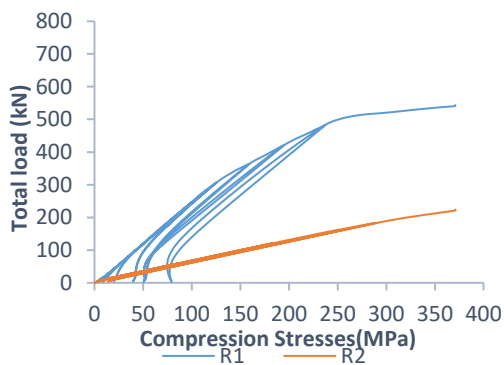


**Figure 25** Maximum Compression tensions at both rosettes

### 5.3 Comparison of the results for V1 and V2

Comparing the results obtained for both beams, it is clear that the reinforcement not only increases the beam's resistance, it also increases its ductility, as shown in figure .

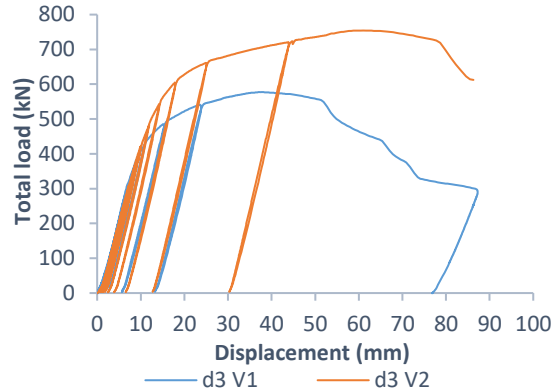


**Figure 26** Comparison of displacement d3 for both beams

In terms of stresses, the results comparison for R1, illustrated on figure 28 show that the maximum principal compressions stresses have a faster growing rate for beam V1, which shows the effect of the reinforcements.

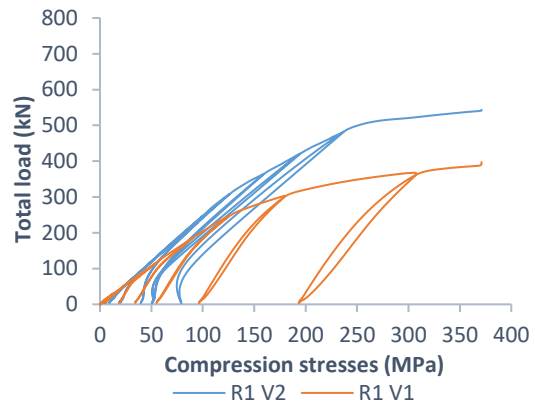


**Figure 27** Comparison of the results at R1 for both beams

On the other hand, for rosette R2, right on the opening's corner, the results for both beams were more similar, showing that the reinforcement's influence is mostly felt between them and the flanges. The results are shown in figure 29.



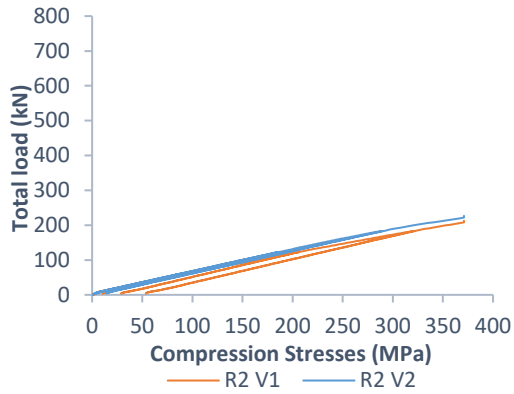


**Figure 28** Comparison of the results at R2 for both beams

## 6 Experimental test vs Numerical model

In this chapter the experimental results are compared to the numerical results, in order to assess the model's behaviour.

### 6.1 Unreinforced steel beam V1

The results comparison for beam V1 show that the model is capable of reproducing the beams elastic behaviour. The comparison of the results is illustrated at figure 30.

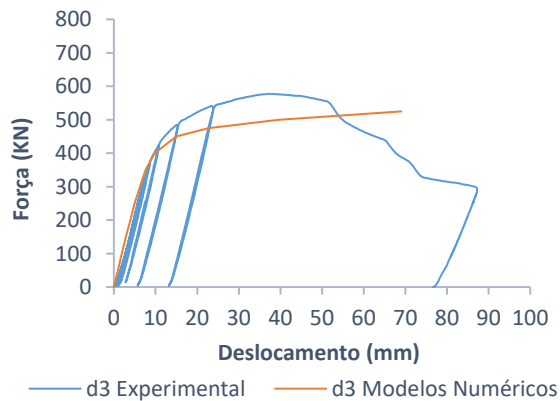


**Figure 29** Comparison of displacement d3 for the numerical model and experimental test

It is also clear that the plastic behavior of the beam is not well reproduced by the model. The software is missing a failure criterion that considers the steel cinematic hardening.

The deformations at the opening registered by the numerical model were also very similar to the experimental ones, as shown in figure 31.

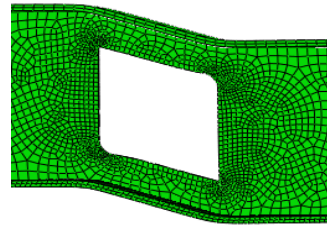


**Figura 30** Deformation at the opening on the numerical model

In terms of stress, the comparison was made for a total load of 200kN, in order to compare the results for numerical and experimental tests. The comparison is shown in table

**Tabela 5** Stress comparison for experimental test and numerical model

Q=200			
Posição	$\sigma_{Exp}$ (MPa)	$\sigma_{Num}$ (MPa)	$\sigma_{Exp}/\sigma_{Num}$
e2(R1)	-60	-75	0,80
e5(R2)	-231	-236	0,98
e10	353	140	2,50
e11	195	202	0,96

As shown the results obtain were mostly very similar for both experimental and numerical analysis.

### 6.2 Reinforced steel beam V2

The results comparison for beam V2 show that the model is capable of reproducing the beams elastic behaviour. The comparison of the results is illustrated at figure 32.

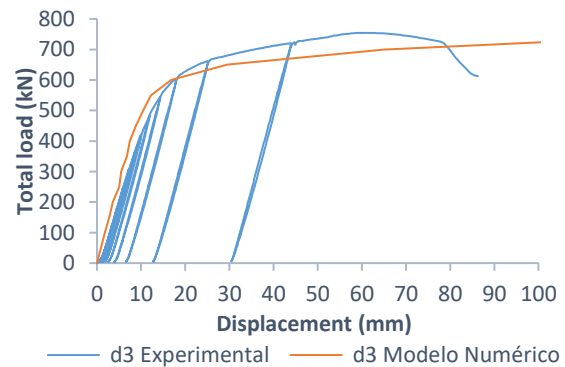


**Figure 31** Comparison of displacement d3 for the numerical model and experimental test

It is also clear that the plastic behavior of the beam is not well reproduced by the model. The software is missing a failure criterion that considers the steel cinematic hardening.

The deformations at the opening registered by the numerical model were also very similar to the experimental ones, as shown in figure 31.

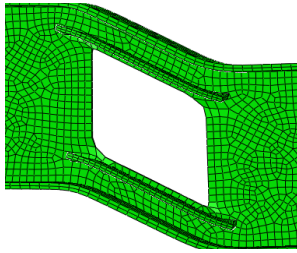


**Figure 32** Deformation at the opening on the numerical model

In terms of stress, the comparison was made for a total load of 250kN, in order to compare the results for numerical and experimental tests. The comparison is shown in table

**Tabela 6** Stress comparison for experimental test and numerical model

Q=250			
Posição	$\sigma_{Exp}$ (Mpa)	$\sigma_{Num}$ (Mpa)	$\sigma_{Exp}/\sigma_{Num}$
e2(R1)	22	20	1,10
e5(R2)	-205	-290	0,71
e10	-	-3	-
e11	231	210	1,10

As shown the results obtain were mostly very similar for both experimental and numerical analysis.

## 7. Conclusions

It is considered that the objectives of these work were achieved. The beams that were tested both failed by the Vierendeel mechanism.

The results obtained by the numerical model are also satisfactory. The beams behaviour in the elastic phase are very similar to the results obtained experimentally.

The reinforcement was also efficient, increasing the beam's loading capacity considerably.

In terms of stresses, it is clear that the reinforcement mostly influences the area between them and the flanges. In the opening's corners the results were very similar for both beams.

## REFERENCES

- [1] CHUNG, K. F., LIU, T. C. H, KO, A. C. H., *Investigation on Vierendeel mechanism in steel beams with circular web openings*, 2001. In: Journal of Constructional Steel Research. Hong Kong: p. 467-490.
- [2] CHUNG, K. F., LIU, T. C. H, KO, A. C. H., *Steel beams with large web openings of various shapes and sizes: an empirical design method using a generalised moment-shear interaction curve*. Em: Journal of Constructional Steel Research. p. 1177-1200, 2003.
- [3] ENV 1992-1-1: 2004, *Design of Concrete Structures-Part 1-1*. Em General Rules and Rules for Buildings,CEN. European Committee for Standardization, 2004.
- [4] ENV 1993-1-1: 2005, *Design of Steel Structures-Part 1-1*. Em General Rules and Rules for Buildings,CEN. European Committee for Standardization, 2005.
- [5] CLAWSON, W. C., DARWIN, D. *Composite Beams with Web Openings*, p. 209. Lawrence, Kansas, 1980.
- [6] BERNARDINO, P. J. C. *Influência de Aberturas nas Almas de Vigas de Aço*, 2013